On the Optimal Power Allocation for Two-Way Full-Duplex AF Relay Networks[§]

Jyun-Wei Li[⋆] and Che Lin[†], *Senior Member, IEEE*

***Abstract*—This paper investigates the optimal power allocation that maximizes the system utility for a full-duplex (FD) amplify-and-forward (AF) two-way relay network (TWRN) with a rate outage and a power constraint. Both cases of an individual and a sum power constraint are considered. To formulate the corresponding optimization problem, closed-form expressions of outage probabilities are needed. With FD transceivers, the derivation of such closed-form expressions become too involved. Thus, approximate closed-form expressions were derived instead. The resulting optimization problem is still non-convex and difficult to solve. Via solving a series of approximate convex problems, a successive convex approximation (SCA) algorithm was proposed. Our simulation results demonstrate the accuracy of the approximate closed-form expressions of outage probabilities and that the proposed SCA algorithm achieves near-optimal performance and significantly outperforms the full power allocation under the individual power constraint and uniform power allocation under the sum power constraint both in system utility and in power consumption. Our results further show that simultaneous power transmission for all relay nodes with judicious power allocation generated by the SCA algorithm achieves 174% of performance gain under the individual power constraint, and 85% of performance gain under the sum power constraint over the relay selection scheme. A tradeoff between the FD system and the half-duplex (HD) system with respect to the residual interference was also observed. We can also observe that not only the residual self-interference but also the cross-link interference is a factor that degrades the system performance for a FD system.**

Index terms— full-duplex systems, two way relay networks, amplify and forward relaying, self-interference, power allocation, utility maximization.

I. Introduction

Cooperative communication has been extensively studied in recent years with different relaying protocols including amplify-and-forward (AF) [1], decode-and-forward (DF) [2], and compress-and-forward (CF) [3] scheme. Among these schemes, AF is the most widely used due to its simplicity. Initial work on the AF scheme focused on one-way relay networks [4]–[6]. To further improve spectral efficiency, two-way relay networks (TWRNs) that utilize the principle of physical layer network coding has been proposed and has attracted attentions among researchers more recently [7]–[13]. An AF-based TWRN utilizes analog network coding (ANC) to support communications in both directions. By using the knowledge of transmitted signals at the terminals and local channel state information (CSI), the number of required transmitted time-slots for one round is reduced from four to two [7]. The network throughput is thus improved. In [8] [9], relay selection schemes have been proposed to realize such improvement in system throughput. The benefit of simultaneous transmission from multiple relays to improve the achievable rate region has been investigated in [10] [11]. Note that each relay in all the aforementioned works is assumed to operate in half-duplex (HD) mode. Thanks to technological progression in recent year, it is now possible to incorporate full-duplex (FD) transceivers into the design of a wireless system [12]. The potential of utilizing FD-enabled transceivers in a TWRN makes simultaneous information exchange between sources possible, i.e., only one time slot is required for the entire two-way communication [13].

Earlier information theoretic studies on FD transceivers in a relay channel have shown its potential performance and capacity benefits [2] [14]. These studies assume perfect self-interference cancellation and can only provide us performance upper bounds. In practice, there is always residual self-interference that reduces the system performance. Several techniques that effectively suppress self-interference have been proposed, such as analog and digital cancellation [15], spatial domain cancellation [16] and code domain cancellation [17]. With these techniques, self-interference can be sufficiently mitigated to allow for possible implementation of FD transceivers in a TWRN.

Initial design of AF schemes with FD transceivers focuses on TWRNs with a single relay node [18] [19]. Riihonen et al. discussed the importance of power control under a dual-hop FD-AF relay system [18]. The optimal power allocation problem was studied under an individual and a global power constraint in [19]. More recently, different relay selection schemes have been studied for a TWRN with multiple relay nodes [20]–[22]. Cui et al. studied the optimal power allocation and the optimal choice of duplex mode based on relay selection [20]. The optimal power allocations that aim to maximize sum rate with different relay selection were studied in [21] [22]. Note that in all the aforementioned works, some type of relay selection scheme is always assumed, i.e., only one relay is allowed to transmit in any given time. In our previous work, we have shown that a significant performance gain is possible by allowing multiple relay nodes to transmit simultaneously, and allocating power appropriately among relay nodes for a TWRN with a HD-AF relaying scheme [11]. It is hence of interest to study whether similar performance gain can be obtained with a FD-AF relaying scheme. This is the focus of our study.

[§] The work is supported by the Ministry of Science and Technology, R.O.C., under Grants MOST104-2221-E-007-041-MY2.

[†] Che Lin is the corresponding author. Address: Institute of Communications Engineering, National Tsing Hua University, Hsinchu, Taiwan 30013, R.O.C. E-mail: clin@ee.nthu.edu.tw.

[⋆] Jyun-Wei Li is with Institute of Communications Engineering, National Tsing Hua University, Hsinchu, Taiwan 30013, R.O.C. E-mail: re21962000@gmail.com

This article has been accepted for publication in a future issue of this journal, but has not been fully edited. Content may change prior to final publication. Citation information: DOI 10.1109/TSP.2017.2736507, IEEE Transactions on Signal Processing

In this paper, we investigate the optimal power allocation that maximizes a general utility function for FD-AF relaying TWRNs under an individual or a sum power constraint. To solve the optimization problem, closed-form expressions of the outage probabilities are needed. Since the derivation of the exact closed-form expressions of outage probabilities are difficult, we derived approximate closed-form expressions of the outage probabilities for both cases of TWRN with a single relay node and multiple relay nodes. Based on the techniques developed in our previous work [23], we propose a successive convex approximation (SCA) algorithm to solve the utility maximization problem under the rate outage constraints. Finally, our simulation results demonstrate the accuracy of our approximation and the superior performance of our proposed algorithm. We list our contributions as follows:

- For a TWRN with FD transceivers, there have been several studies that investigate power allocation to different relay selection schemes [20]–[22]. Instead of applying a relay selection scheme, we investigate the optimal power allocation when all relay nodes are allowed to transmit simultaneously. In fact, we show via simulations that significant performance advantages can be obtained from our proposed power allocation scheme over the relay selection scheme. This study is an extension from our previous work [11] that investigate the optimal power allocation for a HD-AF relaying TWRN. Note that the extension from HD to FD systems is not trivial. Both self-interference and cross-link interference need to be considered in a FD system, leading to a even more complicated optimization problem.
- Since both self-interference and cross-link interference are considered in our model, deriving the closed-form expressions of outage probabilities become even more complicated. Approximation methods are hence needed. We used extensive Monte-Carlo simulations to validate the approximation accuracy of our derived expressions. The resulting utility maximization problem are non-convex and difficult to solve. To deal with these issues, we propose a SCA algorithm to solve the non-convex optimization problem iteratively to obtain high-quality approximate solutions.
- By simulation results, we show that power allocation is an important issue for a FD-AF relaying TWRN with multiple relay nodes. Specifically, simultaneous power transmission from all relay nodes with judicious power allocation generated by our SCA algorithm outperforms the relay selection scheme by as large as 174% under the individual power constraint, and 85% under the sum power constraint when channel is symmetric, indicating the potential benefits to go beyond relay selection schemes. Furthermore, by comparing the utilities achieved by FD and HD systems, we observe that not only the residual self-interference but also the cross-link interference is a factor that degrades the system performance for a FD system. This provides us new insights into the design issues for an FD-AF relaying TWRNs.

Notations: Absolute value is denoted by $|\cdot|$. The phase of a complex variable a is denoted by $\angle a$. $\mathbf{a} \succeq \mathbf{b}$ means $a_i \geq b_i$ component-wise. $\mathbf{x} \sim \mathcal{CN}(\boldsymbol{\mu}, \sigma^{\mathbf{2}})$ means that $\mathbf{x}$ is circularly symmetric complex Gaussian distributed with mean $\boldsymbol{\mu}$ and variance $\sigma^{\mathbf{2}}$. We denote $\exp(\cdot)$ (or simply $e^{(\cdot)}$) by the exponential function, while $\ln(\cdot)$ and $\Pr\{\cdot\}$ stand for the natural log function and the probability function. For a variable a_k, where $k \in \{1, \ldots, K\}$, $\{a_k\}$ denotes the set containing all possible a_k, i.e., $\{a_1, a_2, \ldots, a_K\}$.

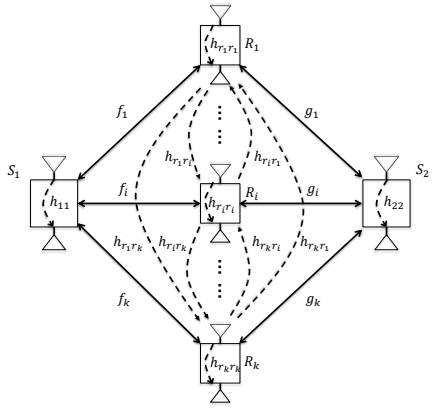

Fig. 1: System model for a two-way full-duplex multi-relay network.

II. System Model and Problem Statement

In this work, we consider a two-way relay amplify-and-forward system with two source nodes, S_1 and S_2, and a cluster of relay nodes R_i, $i = 1, \ldots K$ as depicted in Fig. 1. The two source nodes are interested in exchanging their information. There is no direct link between S_1 and S_2 due to deep fading or heavy shadowing, so the communication must rely on the relay nodes. We assume that each node is equipped with two antennas, one for transmission and the other one for reception of signals. The channels between S_1, S_2 and R_i are denoted by $f_i \sim \mathcal{CN}(0, \sigma^2_{r_i1})$ and $g_i \sim \mathcal{CN}(0, \sigma^2_{r_i2})$, respectively. We assume that the channels between the two source nodes and the relay nodes are reciprocal; i.e., the channels from one source node to the relay nodes, and the channels from the relay nodes to the source node are the same. We assume FD capability for all nodes, resulting in self-interference and cross-link interference for the considered TWRN. We denote the self-interference channels of S_1, S_2, and R_i by $h_{11} \sim \mathcal{CN}(0, \sigma^2_{11})$, $h_{22} \sim \mathcal{CN}(0, \sigma^2_{22})$, and $h_{r_ir_i} \sim \mathcal{CN}(0, \sigma^2_{r_{r_ir_i}})$, respectively. The relays are assumed to interfere with each other. The cross-link interference channel between relays is denoted by $h_{r_ir_j} \sim \mathcal{CN}(0, \sigma^2_{r_{r_ir_j}})$, representing the interference from R_i to R_j for $j = 1, \ldots K$, $j \neq i$. We denote the residual self-interference channel at the i-th relay node as $\tilde{h}_{r_ir_i}$ after analog/digital self-interference cancellation techniques [15]. The statistics of the residual self-interference channel are not well understood yet [24]. The experimental-based study in [25] has demonstrated that the amount of self-interference suppression achieved by a combined analog/digital cancellation technique is a complicated function of several system

parameters. To have a tractable power allocation problem, we model the residual self-interference channel at the i-th relay node as $\tilde{h}_{r_ir_i} \sim \mathcal{CN}(0, \tilde{\sigma}^2_{r_ir_i})$ [26]. We assume that all channels are statistically independent, frequency flat, and remain constant for a transmission block. In addition, there is local channel state information at the receiver end (CSIR) for all nodes. When S_1 serves as a transmitter and transmits signal to R_i, R_i can obtain the CSI information of f_i via training. Now when S_2 serves as a transmitter, R_i can obtain the CSI information of g_i when it receives training signals from S_2 in the training stage. In conclusion, R_i can learn about local CSIR of f_i and g_i from S_1 and S_2, respectively. The network also consists of a control center which has global channel distribution information (CDI) and solves the optimal power allocation to all nodes.

When operating in FD mode, the two source nodes and all relay nodes transmit and receive simultaneously. The source nodes and the relay nodes are assumed to be perfectly synchronized. The received signal at the i-th relay node can be expressed as

$$y_{r_i}[m] = f_i s_1[m] + g_i s_2[m] + h_{r_ir_i} x_{r_i}[m] + \sum_{j=1, j\neq i}^{K} h_{r_jr_i} x_{r_j}[m] + n_{r_i}[m],\ i = 1, \cdots, K, \tag{1}$$

where $s_1[m]$ and $s_2[m]$ are the transmitted signals from S_1 and S_2 at time m, and $n_{r_i}[m]$ is the additive white Gaussian noise (AWGN) with unit variance at the i-th relay node. The i-th relay node applies AF protocol and multiplies the received signal with a complex coefficient w_{r_i} before transmission, i.e., $x_{r_i}[m] = w_{r_i} y_{r_i}[m-1]$. Furthermore, the self-interference, caused by the FD mode, can be suppressed by analog/digital self-interference cancellation techniques [15] but perfect cancellation cannot be done due to practical constraints. Thus, the received signal in (1) can be represented as

$$y_{r_i}[m] = f_i s_1[m] + g_i s_2[m] + \tilde{h}_{r_ir_i} x_{r_i}[m] + \sum_{j=1, j\neq i}^{K} h_{r_jr_i} x_{r_j}[m] + n_{r_i}[m], i = 1, \cdots, K, \tag{2}$$

where $\tilde{h}_{r_ir_i} \sim \mathcal{CN}(0, \tilde{\sigma}^2_{r_ir_i})$ is the residual self-interference channel at the i-th relay node.

Next, observe the received signal at the source nodes

$$y_1[m] = \sum_{i=1}^{K} f_i x_{r_i}[m] + h_{11} s_1[m] + n_1[m], \tag{3a}$$

$$y_2[m] = \sum_{i=1}^{K} g_i x_{r_i}[m] + h_{22} s_2[m] + n_2[m], \tag{3b}$$

where $n_1[m]$ and $n_2[m]$ are AWGN with unit variance at S_1 and S_2. As mentioned before, we can suppress the self-interference signal at S_1 and S_2 by using self-interference cancellation techniques, but the residual self-interference still remains. Plugging in the expression of $x_{r_i}[m]$, we obtain

$$y_1 = \sum_{i=1}^{K} f_i w_{r_i} (f_i s_1[m-1] + g_i s_2[m-1] + \tilde{h}_{r_ir_i} x_{r_i}[m-1] + \sum_{j=1, j\neq i}^{K} h_{r_jr_i} x_{r_j}[m-1] + n_{r_i}[m-1]) + \tilde{h}_{11} s_1[m] + n_1[m], \tag{4a}$$

$$y_2 = \sum_{i=1}^{K} g_i w_{r_i} (f_i s_1[m-1] + g_i s_2[m-1] + \tilde{h}_{r_ir_i} x_{r_i}[m-1] + \sum_{j=1, j\neq i}^{K} h_{r_jr_i} x_{r_j}[m-1] + n_{r_i}[m-1]) + \tilde{h}_{22} s_2[m] + n_2[m]. \tag{4b}$$

where $\tilde{h}_{11} \sim \mathcal{CN}(0, \tilde{\sigma}^2_{11})$ and $\tilde{h}_{22} \sim \mathcal{CN}(0, \tilde{\sigma}^2_{22})$ are the residual self-interference channels at the source nodes. Although the AF coefficients $\{w_{r_i}\}_{i=1}^K$ are not known by the source nodes, we assume that the relay nodes can inform S_1 and S_2 the value of $\{w_{r_i}\}_{i=1}^K$. Since $s_1[m-1]$ and $s_2[m-1]$ is also respectively known at S_1 and S_2, they can be cancelled and the remaining signals become

$$y_1 = \sum_{i=1}^{K} f_i w_{r_i} (g_i s_2[m-1] + \tilde{h}_{r_ir_i} x_{r_i}[m-1] + \sum_{j=1, j\neq i}^{K} h_{r_jr_i} x_{r_j}[m-1] + n_{r_i}[m-1]) + \tilde{h}_{11} s_1[m] + n_1[m], \tag{5a}$$

$$y_2 = \sum_{i=1}^{K} g_i w_{r_i} (f_i s_1[m-1] + \tilde{h}_{r_ir_i} x_{r_i}[m-1] + \sum_{j=1, j\neq i}^{K} h_{r_jr_i} x_{r_j}[m-1] + n_{r_i}[m-1]) + \tilde{h}_{22} s_2[m] + n_2[m]. \tag{5b}$$

We assume that the source signals s_1 and s_2 are Gaussian encoded with distribution $\mathcal{CN}(0,1)$. Thus, the instantaneous achievable rate Γ_1, Γ_2 for S_1 and S_2 can be characterized as

$$\Gamma_1 = \log_2 \left(1 + \frac{P_2 (\sum_{i=1}^K |f_i g_i| |w_{r_i}|)^2}{\sum_{i=1}^K P_{r_i} |f_i|^2 |\tilde{h}_{r_ir_i}|^2 |w_{r_i}|^2 + \sum_{i=1}^K |f_i|^2 |w_{r_i}|^2} \right.$$
$$\left. \frac{}{+ \sum_{i=1}^K |f_i|^2 |w_{r_i}|^2 \sum_{j=1, j\neq i}^K P_{r_j} |h_{r_jr_i}|^2 + P_1 |\tilde{h}_{11}|^2 + 1} \right), \tag{6a}$$

$$\Gamma_2 = \log_2 \left(1 + \frac{P_1 (\sum_{i=1}^K |f_i g_i| |w_{r_i}|)^2}{\sum_{i=1}^K P_{r_i} |g_i|^2 |\tilde{h}_{r_ir_i}|^2 |w_{r_i}|^2 + \sum_{i=1}^K |g_i|^2 |w_{r_i}|^2} \right.$$
$$\left. \frac{}{+ \sum_{i=1}^K |g_i|^2 |w_{r_i}|^2 \sum_{j=1, j\neq i}^K P_{r_j} |h_{r_jr_i}|^2 + P_2 |\tilde{h}_{22}|^2 + 1} \right), \tag{6b}$$

where P_1, P_2, and P_{r_i} are the transmitted power at S_1, S_2, and R_i, respectively. Note that the time index is removed for notational simplicity. As mentioned earlier, we assumed that local CSIR is available at all relay nodes, i.e., f_i and g_i are known to R_i. Therefore, the phase of the AF coefficients for R_i can be chosen as $\angle w_{r_i} = -\angle f_i - \angle g_i$ to cancel out phase shift caused by the fading coefficients.

In this paper, our goal is to investigate a utility maximization problem. We consider the following system utility function as the objective function in our optimization problem [27]:

$$U_\beta(\{R_i\}) = \begin{cases} \sum_{i=1}^N \frac{\alpha_i R_i^{1-\beta}}{1-\beta}, & 0 \leq \beta < \infty, \beta \neq 1, \\ \sum_{i=1}^N \alpha_i \ln(R_i), & \beta = 1, \end{cases} \tag{7}$$

where the coefficients $\alpha_i \in [0,1]$ for $i = 1, \cdots, N$ with $\sum_{i=1}^N \alpha_i = 1$ represent the user priority, and the parameter $\beta \in [0, \infty)$ represents user fairness. For example, for β being 0, 1, 2, $U_\beta(\{R_i\})$ corresponds to weighted sum rate, weighted geometric mean rate, and weighted harmonic mean

This article has been accepted for publication in a future issue of this journal, but has not been fully edited. Content may change prior to final publication. Citation information: DOI 10.1109/TSP.2017.2736507, IEEE Transactions on Signal Processing

rate, respectively. It can be shown that $U_\beta(\{R_i\})$ is concave in $\{R_i\}$ for any value of β. Furthermore, we consider outage probability constraints as quality-of-service (QoS) constraints for our considered optimization problem [11]. We also consider both cases of individual and sum power constraint in our problem settings. When an individual power constraint is considered, we have $\Omega_p^i = \{\{P_j\}_{j=1}^K | P_j \leq \bar{P}_j, j = 1, \cdots, K\}$, where $\bar{P}_j$ is an upper bound on the individual power. When a sum power constraint is considered, we have $\Omega_p^s = \{\{P_j\}_{j=1}^K | \sum_{j=1}^K P_j \leq P_T\}$, where P_T is an upper bound on the total sum power. Then, our considered utility maximization problem is given by

$$\max_{\{\{P_{r_i}\}_{i=1}^K, P_1, P_2, R_1, R_2\} \succeq 0} \quad U(R_1, R_2) \tag{8a}$$

$$\text{s.t.} \quad \Pr(\Gamma_1 < R_1) \leq \epsilon_1, \tag{8b}$$

$$\Pr(\Gamma_2 < R_2) \leq \epsilon_2, \tag{8c}$$

$$\{\{P_{r_i}\}_{i=1}^K, P_1, P_2\} \in \Omega_p^i \text{ or } \Omega_p^s, \tag{8d}$$

where $\epsilon_m \in [0, 1]$ is the maximum tolerable outage probability for the m-th receiver for $m = 1, 2$. Note that diversity order is not considered in this work. Usually, diversity order is considered in the high SNR case. Here, we consider a practical SNR level where the peak power constraint of relay node and source nodes is set to 30 W and the noise power is set to 1 W in simulations. Instead of minimizing outage probability (or maximizing diversity order for high SNR), the outage probabilities are considered as constraints here while the system utility is maximized. To solve the utility maximization problem, we need to obtain closed-form expressions for of the outage probabilities. Due to the complicated structure of outage probabilities, we apply approximation methods to derive their approximate closed-form expressions.

III. Approximate Closed-Form Expressions for Outage Probabilities

In this section, we use approximation methods to derive closed-form expressions of outage probabilities. We consider two different cases: a TWRN with a single relay node and multiple relay nodes. We applied different AF coefficients of relay nodes to obtain tractable closed-form expressions of outage probabilities for both cases. As it will become clear later, we need further assumptions and modifications to the AF coefficients when there are multiple relay nodes. The outage probabilities can be obtained by substituting the instantaneous achievable rate Γ_1 and Γ_2 into (8b) and (8c), respectively. For simplicity, we only demonstrate the derivation of the approximate outage probability for S_1. The derivation for S_2 can be obtained with the same procedure.

A. Single Relay Node

Now, we derive approximate closed-form expressions of outage probabilities for a TWRN with a single relay node. Note that there is only one relay node in this setting. Thus, there is no cross-link interference between relays. Since local CSIR is available at the relay node, the AF coefficient of relay node can be designed as

$$w_{r_1} = \frac{\sqrt{P_{r_1}} e^{j(-\angle f_1 - \angle g_1)}}{\sqrt{P_1 |f_1|^2 + P_2 |g_1|^2 + P_{r_1} |\tilde{h}_{r_1 r_1}|^2 + 1}}. \tag{9}$$

The term in the denominator is used to normalize the instantaneous received power at the relay node. Then, we can calculate the effective signal to interference plus noise ratio (SINR) and obtain the outage probability at S_1 as

$$\Pr\left(\frac{|f_1|^2 |g_1|^2 P_{r_1} P_2}{|f_1|^2 (|\tilde{h}_{r_1 r_1}|^2 P_{r_1}^2 + P_{r_1} + |\tilde{h}_{11}|^2 P_1^2 + P_1) + |g_1|^2 (|\tilde{h}_{11}|^2 P_1 P_2 + P_2)} \right.$$
$$\left. \frac{}{+ (P_1 |\tilde{h}_{11}|^2 + 1)(P_{r_1} |\tilde{h}_{r_1 r_1}|^2 + 1)} < 2^{R_1} - 1 \right). \tag{10}$$

Harmonic-to-mean (HMA) approximation [28] is used to derive the approximate closed-form expression. To begin with, we divide both the numerator and denominator of the effective SINR of (10) by $(P_1 \tilde{\sigma}_{11}^2 + 1)(P_{r_1} |\tilde{h}_{r_1 r_1}|^2 + 1)$. Then, the outage probability in (10) can be rewritten as

$$\Pr\left(\frac{\frac{|f_1|^2 |g_1|^2 P_{r_1} P_2}{(P_1 \tilde{\sigma}_{11}^2 + 1)(P_{r_1} |\tilde{h}_{r_1 r_1}|^2 + 1)}}{\frac{|f_1|^2 (|\tilde{h}_{r_1 r_1}|^2 P_{r_1}^2 + P_{r_1} + 2 P_1^2 \tilde{\sigma}_{11}^2 + P_1)}{(P_1 \tilde{\sigma}_{11}^2 + 1)(P_{r_1} |\tilde{h}_{r_1 r_1}|^2 + 1)} + \frac{|g_1|^2 (2 P_2 P_1 \tilde{\sigma}_{11}^2 + P_2)}{(P_1 \tilde{\sigma}_{11}^2 + 1)(P_{r_1} |\tilde{h}_{r_1 r_1}|^2 + 1)} + 1} < 2^{R_1} - 1 \right), \tag{11}$$

Here, we approximate residual self-interference channel at the source nodes to their respective means, i.e., $|\tilde{h}_{11}|^2 \approx \tilde{\sigma}_{11}^2$. Next, we apply a harmonic-to-mean approximation (HMA) method, expressed as $\frac{xy}{x+y} = \frac{1}{\frac{1}{x} + \frac{1}{y}} \leq \min\{x, y\}$ [28]. The approximation is done by first neglecting 1 in the denominator since it has small effect to the outage performance [20], and then by applying the HMA method. Thus, the outage probability in (11) can be approximated as

$$\Pr\left(P_{r_1} \min\left\{ \frac{|f_1|^2}{P_1 \tilde{\sigma}_{11}^2 + 1}, \frac{|g_1|^2 P_2}{|\tilde{h}_{r_1 r_1}|^2 P_{r_1}^2 + P_{r_1} + P_1^2 \tilde{\sigma}_{11}^2 + P_1} \right\} < 2^{R_1} - 1 \right) \tag{12}$$

Then, we can obtain the approximate closed-form expressions of outage probability for a single relay node as

$$\Pr(\Gamma_1 < R_1) \approx 1 - \left(\frac{1}{1 + \frac{(2^{R_1} - 1) P_{r_1} \tilde{\sigma}_{r_1 r_1}^2}{P_2 \sigma_{r_1 2}^2}} \right) \cdot$$
$$\exp\left(- \left(\frac{P_1 \tilde{\sigma}_{11}^2 + 1}{P_{r_1} \sigma_{r_1 1}^2} + \frac{P_{r_1} + P_1^2 \tilde{\sigma}_{11}^2 + P_1}{P_2 P_{r_1} \sigma_{r_1 2}^2} \right) \left(2^{R_1} - 1 \right) \right). \tag{13}$$

B. Multiple Relay Nodes

In this subsection, we derive closed-form expressions of outage probabilities for a TWRN with multiple relay nodes. Since there is a product of two channel coefficients appearing in the numerator of (8b) and (8c) by substituting r_1 and r_2, respectively, the derivation of outage probabilities is difficult. For this, we adopt different AF coefficients when there are multiple relay nodes. Specifically, we design the AF coefficients as

$$w_{r_i} = \frac{\sqrt{P_{r_i}} e^{j(-\angle f_1 - \angle g_1)}}{\sqrt{N_{r_i}}} \frac{1}{|f_i||g_i|}, \tag{14}$$

where N_{r_i} is used to normalize the long-term transmitted power at the i-th relay node to P_{r_i} such that it is possible to obtain a tractable closed-form expressions of outage probabilities. Then, the transmitted signal at the i-th relay node can be represented as

$$x_{r_i} = \sqrt{\frac{P_{ri}}{N_{r_i}}} \left(\frac{s_1}{g_i} + \frac{s_2}{f_i} + \frac{\tilde{h}_{r_i r_i} x_{r_i}}{f_i g_i} + \frac{\sum_{j=1, j\neq i}^{K} h_{r_j r_i} x_{r_j}}{f_i g_i} + \frac{n_{r_i}}{f_i g_i} \right), \tag{15}$$

and N_{r_i} can be calculated by letting $\mathbb{E}[|x_{r_i}|^2]$ equal to P_{r_i}, i.e.,

$$N_{r_i} = \mathbb{E}\left[\frac{1}{|g_i|^2}\right] P_1 + \mathbb{E}\left[\frac{1}{|f_i|^2}\right] P_2 + \mathbb{E}\left[\frac{1}{|f_i|^2}\right] \mathbb{E}\left[\frac{1}{|g_i|^2}\right] \left(P_{r_i} \mathbb{E}\left[|\tilde{h}_{r_i r_i}|^2\right] + \sum_{j=1, j\neq i}^{K} P_{r_j} \mathbb{E}\left[|h_{r_j r_i}|^2\right] + 1 \right). \tag{16}$$

Note that the terms $\frac{1}{|f_i|^2}$ and $\frac{1}{|g_i|^2}$ are inverse gamma distributed random variables. The expectations of both $\frac{1}{|f_i|^2}$ and $\frac{1}{|g_i|^2}$ are infinite for the reason that the probability density functions (PDF) approach zero very slowly when the random variables $\frac{1}{|g_i|^2}$ and $\frac{1}{|f_i|^2}$ approach to infinity. To avoid such issue, we propose a scheme in which the relay nodes would not forward the signal if $|f_i|^2 < \eta$ or $|g_i|^2 < \eta$, where η is a small positive constant and is defined as the *channel truncation level*.

With the above scheme, we can derive the expectations $\mathbb{E}\left[\frac{1}{|g_i|^2} \middle| |g_i|^2 \geq \eta\right]$ and $\mathbb{E}\left[\frac{1}{|f_i|^2} \middle| |g_i|^2 \geq \eta\right]$. Therefore, N_{r_i} can be express as

$$N_{r_i} = \frac{1}{\sigma^2_{r_i 2}} \mathbf{E}_1\left(\frac{\eta}{\sigma^2_{r_i 2}}\right) e^{\frac{\eta}{\sigma^2_{r_i 2}}} P_1 + \frac{1}{\sigma^2_{r_i 1}} \mathbf{E}_1\left(\frac{\eta}{\sigma^2_{r_i 1}}\right) e^{\frac{\eta}{\sigma^2_{r_i 1}}} P_2 + \frac{1}{\sigma^2_{r_i 1}} \mathbf{E}_1\left(\frac{\eta}{\sigma^2_{r_i 1}}\right) e^{\frac{\eta}{\sigma^2_{r_i 1}}} \frac{1}{\sigma^2_{r_i 2}} \mathbf{E}_1\left(\frac{\eta}{\sigma^2_{r_i 2}}\right) e^{\frac{\eta}{\sigma^2_{r_i 2}}} \left(P_{r_i} \tilde{\sigma}^2_{r_i r_i} + \sum_{j=1, j\neq i}^{K} P_{r_j} \sigma^2_{r_j r_i} + 1 \right), \tag{17}$$

where $\mathbf{E}_1(\cdot)$ is the exponential integral function. Substituting N_{r_i} into (14), we can obtain the AF coefficients for the relay nodes. Then, we can further calculate the corresponding outage probability as

$$\Pr\left(\frac{P_2 \left(\sum_{i=1}^{K} \sqrt{\frac{P_{r_i}}{N_{r_i}}}\right)^2}{\sum_{i=1}^{K} \frac{P^2_{r_i}}{N_{r_i}} \frac{|\tilde{h}_{r_i r_i}|^2}{|g_i|^2} + \sum_{i=1}^{K} \frac{P_{r_i}}{N_{r_i}} \frac{1}{|g_i|^2} \sum_{j=1, j\neq i}^{K} P_{r_j} |h_{r_j r_i}|^2 + \sum_{i=1}^{K} \frac{P_{r_i}}{N_{r_i}} \frac{1}{|g_i|^2} + P_1 |\tilde{h}_{11}|^2 + 1} < 2^{R_1} - 1 \middle| |g_1|^2, \ldots, |g_K|^2 > \eta \right). \tag{18}$$

Here, a generalized HMA method is used to derive the approximate closed-form expression. Similarly, we approximate self-interference at the source nodes to their respective means. Thus, (18) can be approximated as

$$\Pr\left(\frac{P_2 \left(\sum_{i=1}^{K} \sqrt{\frac{P_{r_i}}{N_{r_i}}}\right)^2}{\sum_{i=1}^{K} \frac{P^2_{r_i}}{N_{r_i}} \frac{|\tilde{h}_{r_i r_i}|^2}{|g_i|^2} + \sum_{i=1}^{K} \frac{P_{r_i}}{N_{r_i}} \frac{1}{|g_i|^2} \sum_{j=1, j\neq i}^{K} P_{r_j} |h_{r_j r_i}|^2 + \sum_{i=1}^{K} \frac{P_{r_i}}{N_{r_i}} \frac{1}{|g_i|^2} + P_1 \tilde{\sigma}^2_{11} + 1} < 2^{R_1} - 1 \middle| |g_1|^2, \ldots, |g_K|^2 > \eta \right). \tag{19}$$

Then, we apply the generalized HMA method for further approximation. The generalized HMA method can be written as $\frac{1}{\frac{1}{x_1} + \frac{1}{x_2} + \ldots + \frac{1}{x_K}} \leq \min\{x_1, x_2, \ldots, x_K\}$. To obtain the form of the general HMA method, we keep the terms associated with $\frac{1}{|g_i|^2}$ in the denominator on the left side of the inequality, and move all other terms to the right side of the inequality. Then, the outage probability in (19) can be represented as

$$\Pr\left(\frac{1}{\sum_{i=1}^{K} \left(\frac{P^2_{ri}}{N_{r_i}} |\tilde{h}_{r_i r_i}|^2 + \frac{P_{r_i}}{N_{r_i}} \sum_{j=1, j\neq i}^{K} P_{r_j} |h_{r_j r_i}|^2 + \frac{P_{r_i}}{N_{r_i}} \right) \frac{1}{|g_i|^2}} < u_1 \triangleq \frac{2^{R_1} - 1}{P_2 \left(\sum_{l=1}^{K} \sqrt{\frac{P_{r_l}}{N_{r_l}}}\right)^2 - \left(2^{R_1} - 1\right)\left(P_1 \tilde{\sigma}^2_{11} + 1\right)} \middle| |g_1|^2, \ldots, |g_K|^2 > \eta \right), \tag{20}$$

Now, the outage probability in (20) can be approximated by the general HMA method as

$$\Pr\left(\min\left\{ \frac{|g_i|^2}{\frac{P^2_{r_i}}{N_{r_i}} |\tilde{h}_{r_i r_i}|^2 + \frac{P_{r_i}}{N_{r_i}} \sum_{j=1, j\neq i}^{K} P_{r_j} |h_{r_j r_i}|^2 + \frac{P_{r_i}}{N_{r_i}}} \right\}_{i=1}^{K} < u_1 \middle| |g_1|^2, \ldots, |g_K|^2 > \eta \right), \tag{21}$$

Then, the approximate closed-form expressions of outage probability can be calculated as

$$1 - \prod_{i=1}^{K} \left(\frac{1}{1 + \frac{P^2_{r_i} u_1 \tilde{\sigma}^2_{r_i r_i}}{N_{r_i} \sigma^2_{r_i 2}}} \prod_{j=1, j\neq i}^{K} \frac{1}{1 + \frac{P_{r_i} P_{r_j} u_1 \sigma^2_{r_j r_i}}{N_{r_i} \sigma^2_{r_i 2}}} \exp\left(-\frac{P_{r_i} u_1}{N_{r_i} \sigma^2_{r_i 2}} + \frac{\eta}{\sigma^2_{r_i 2}} \right) \right). \tag{22}$$

Since η is usually chosen to be a small constant, we can further conservatively approximate the outage probability as

$$\Pr(\Gamma_1 < R_1) \approx 1 - \prod_{i=1}^{K} \left(\frac{1}{1 + \frac{P^2_{r_i} u_1 \tilde{\sigma}^2_{r_i r_i}}{N_{r_i} \sigma^2_{r_i 2}}} \cdot \prod_{j=1, j\neq i}^{K} \frac{1}{1 + \frac{P_{r_i} P_{r_j} u_1 \sigma^2_{r_j r_i}}{N_{r_i} \sigma^2_{r_i 2}}} \exp\left(-\frac{P_{r_i} u_1}{N_{r_i} \sigma^2_{r_i 2}} \right) \right), \tag{23}$$

where $u_m \triangleq \frac{2^{R_m} - 1}{P_n \left(\sum_{l=1}^{K} \sqrt{\frac{P_{r_l}}{N_{r_l}}}\right)^2 - (2^{R_m} - 1)(2 P_m \tilde{\sigma}^2_{mm} + 1)}$, for $m = 1, 2,\ n \in \{1, 2\} \setminus \{m\}$.

Now, we obtain approximate closed-form expressions of outage probabilities for both cases of TWRN with a single relay node and multiple relay nodes. We further investigate the approximation accuracy in the following subsection.

C. Approximation Accuracy

In this subsection, we use Monte Carlo simulations to demonstrate the approximation accuracy of our derived closed-form expressions. Fig. 2(a) and Fig. 2(b) demonstrate the comparison between Monte-Carlo simulations and our derived expressions for a single relay node and multiple relay nodes,

This article has been accepted for publication in a future issue of this journal, but has not been fully edited. Content may change prior to final publication. Citation information: DOI 10.1109/TSP.2017.2736507, IEEE Transactions on Signal Processing

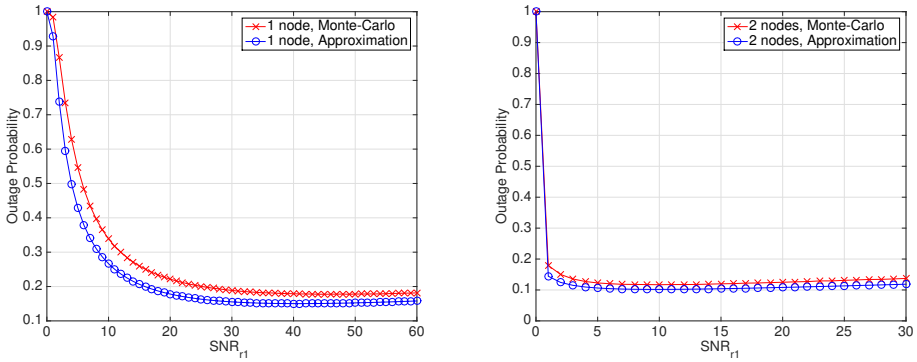

(a) (b)

Fig. 2: Comparison between the Monte-Carlo simulations and approximate closed-form expressions of outage probability with the variance of P_{r_1}, the noise power at R_1 being set to 1 W; (a) single relay node. (b) multiple relay nodes.

respectively. Each Monte-Carlo simulation is obtained by averaging over 10^7 channel realizations of f_i, g_i, $\tilde{h}_{11}$, $\tilde{h}_{22}$, $\tilde{h}_{r_i r_i}$, and $h_{r_i r_j}$ for $i = 1, \dots K$, $i \neq j$. We consider $K = 2$ to observe the approximation accuracy for multiple relay nodes. Note that we have done extensive simulation results for different parameters to check the approximation accuracy. Only two examples are included here due to space constraint. The parameter setting is as follows: We fix the power of S_1 and S_2 as 30 Watt (W). The *channel truncation level* η is set to 0.001. Furthermore, the variance of f_i and g_i are set to 1. We set the variance of residual self-interference channels to 0.01 and 0.05 for source nodes and relay nodes, respectively. The variance of cross-link interference channels are set to 0.1, and the value of R_1 and R_2 are fixed to 1.

We observe the approximation accuracy for P_{r_1} varying from 0 W to 60 W in Fig. 2(a). The difference between the approximation and the Monte-Carlo simulations is about 0.07 around $P_{r_1} = 10W$. In Fig. 2(b), only P_{r_1} is varied with P_{r_2} fixed to 30 W. We can observe even better approximation accuracy when P_{r_1} is varied. The above two examples illustrate the accuracy of our approximations, which is further verified via extensive simulations. Note that in our utility maximization problem, outage probability is considered as a QoS constraint and it can be viewed as a lower bound on symbol error probability (SEP). The figure further showed how outage probability varies with SNR for relay r_1 for both the single and multiple relay nodes cases.

IV. Optimization Problem for FD Two-Way Relay Channels

In this section, we consider two different optimization problems for a TWRN, one with a single relay node and the other with multiple relay nodes. As mentioned before, the optimization problem can be written as (8). Our goal is to solve the utility maximum problem for a TWRN under an individual or a sum power constraint. Unfortunately, both problem are non-convex and cannot be solved efficiently by standard convex solvers such as CVX [29]. In this section, we use some approximation methods to obtain an approximate convex problem. To further improve the quality of our solution, we propose a successive convex approximation (SCA) algorithm [23].

A. SCA Algorithm for a Single Relay Node

In this subsection, we consider the utility maximum problem for a TWRN with a single relay node under an individual and a sum power constraint. With approximate closed-form expressions of outage probabilities derived in Subsection (III-A), the optimization problem for a single relay node can be represented as

$$\max_{(P_m, P_{r_1}, R_1, R_2) \succeq 0} U(R_1, R_2) \tag{24a}$$

$$\text{s.t.} \quad \exp\left(\left(\frac{P_m \tilde{\sigma}^2_{mm} + 1}{P_{r_1}\sigma^2_{r_1 m}} + \frac{P_{r_1} + P_m^2 \tilde{\sigma}^2_{mm} + P_m}{P_l P_{r_1} \sigma^2_{r_1 l}}\right)\left(2^{R_m} - 1\right)\right)$$
$$\left(1 + \frac{\left(2^{R_m} - 1\right) P_{r_1} \tilde{\sigma}^2_{r_1 r_1}}{P_l \sigma^2_{r_1 l}}\right) \leq \frac{1}{1 - \epsilon_m}, \tag{24b}$$

$$\{P_m, P_{r_1}\} \in \Omega_p^s \text{ or } \Omega_p^i, \tag{24c}$$

for $m = 1, 2,\ l \in \{1, 2\} \setminus \{m\}$. We observe that problem (24) is non-convex due to constraint (24b). To handle this, we consider the following change of variables

$$e^{x_{r_1,u}} \triangleq P_{r_1}, e^{x_{r_1,d}} \triangleq P_{r_1}, e^{x_{m,u}} \triangleq P_m, e^{x_{m,d}} \triangleq P_m,$$
$$e^{y_m} \triangleq 2^{R_m} - 1,\ m = 1, 2, \tag{25}$$

where $x_{r_1,u}, x_{r_1,d}, x_{m,u}, x_{m,d}, y_m$ are slack variables. Note that we change the variables of P_m and P_{r_1} twice. This is because P_m and P_{r_1} have different trends in different equations. Specifically, $x_{r_1,u}$, $x_{m,u}$ are the higher the better while $x_{r_1,d}$, $x_{m,d}$ are the lower the better for the utility optimization problem. By substituting (25) into (24), we can reformulate problem (24) as

$$\max_{\substack{(R_1,R_2)\succeq 0,\\ x_{m,u},x_{m,d}\\ ,x_{r_1,u},x_{r_1,d},y_m\in\mathbb{R}}} \quad U(R_1,R_2) \tag{26a}$$

$$\text{s.t.} \quad \exp\left(\frac{\tilde{\sigma}_{mm}^2}{\sigma_{r_1 m}^2}e^{y_m+x_{m,d}-x_{r_1,u}}+\frac{1}{\sigma_{r_1 m}^2}e^{y_m-x_{r_1,u}}+\frac{1}{\sigma_{r_1 l}^2}e^{y_m-x_{l,u}}+\right.$$
$$\left.\frac{\tilde{\sigma}_{mm}^2}{\sigma_{r_1 l}^2}e^{y_m+2x_{m,d}-x_{l,u}-x_{r_1,u}}+\frac{1}{\sigma_{r_1 l}^2}e^{y_m+x_{m,d}-x_{l,u}-x_{r_1,u}}\right).$$
$$\left(1+\frac{\tilde{\sigma}_{r_1 r_1}^2}{\sigma_{r_1 l}^2}e^{y_m+x_{r_1,d}-x_{l,u}}\right)\le\frac{1}{1-\epsilon_m}, \tag{26b}$$
$$R_m\le\log_2\left(1+e^{y_m}\right), \tag{26c}$$
$$e^{x_{r_1,u}}\le P_{r_1}, \tag{26d}$$
$$e^{x_{r_1,d}}\ge P_{r_1}, \tag{26e}$$
$$e^{x_{m,u}}\le P_m, \tag{26f}$$
$$e^{x_{m,d}}\ge P_m, \tag{26g}$$
$$\{e^{x_{m,u}},e^{x_{m,d}},e^{x_{r_1,u}},e^{x_{r_1,d}}\}\in\Omega_p^s \text{ or } \Omega_p^i. \tag{26h}$$

Note that we replace equalities in (26) with inequalities in (26c)-(26g), which is a relaxation of the original constraints. It can be verified by contradiction that the inequality constraints (26b)-(26g) would hold with equalities at the optimal point. The constraints (26b), (26d), and (26f) are now convex. However, (26c), (26e), and (26g) are still non-convex constraints. To handle these non-convex constraints, we introduce a set of first-order approximations, which is a set of conservative approximations. To begin with, we let $(\bar{R}_1,\ \bar{R}_2,\ \bar{P}_m,\ \bar{P}_{r_1})$ be a feasible point to the problem (26). With the feasible point, we define

$$\bar{y}_m\triangleq\ln(2^{\bar{R}_m}-1),\bar{x}_{m,d}\triangleq\ln(\bar{P}_m),\bar{x}_{r_1,d}\triangleq\ln(\bar{P}_{r_1}), \tag{27}$$

for $m=1,2$. We approximate (26c), (26e), and (26g) at the point $(\bar{y}_m,\bar{x}_{m,d},\bar{x}_{r_1,d})$ via first-order approximations, which are a lower bound to the original function. Then, we obtain an approximate problem for (24), which can be represented as (28). Problem (28) is now a convex optimization problem. It can be solved efficiently by standard convex solvers such as CVX. Let $(\hat{R}_1,\hat{R}_2,\hat{x}_{m,u},\hat{x}_{m,d},\hat{x}_{r_1,u},\hat{x}_{r_1,d})$ denote the optimal solution to (28). Since the first-order approximation is a conservative approximation, it would shrink the feasible set of the original problem (24).

$$\max_{\substack{(R_1,R_2)\succeq 0,\\ x_{m,u},x_{m,d}\\ ,x_{r_1,u},x_{r_1,d},y_m\in\mathbb{R}}} \quad U(R_1,R_2) \tag{28a}$$

$$\text{s.t.} \quad \exp\left(\frac{\tilde{\sigma}_{mm}^2}{\sigma_{r_1 m}^2}e^{y_m+x_{m,d}-x_{r_1,u}}+\frac{1}{\sigma_{r_1 m}^2}e^{y_m-x_{r_1,u}}+\frac{1}{\sigma_{r_1 l}^2}e^{y_m-x_{l,u}}+\right.$$
$$\left.\frac{\tilde{\sigma}_{mm}^2}{\sigma_{r_1 l}^2}e^{y_m+2x_{m,d}-x_{l,u}-x_{r_1,u}}+\frac{1}{\sigma_{r_1 l}^2}e^{y_m+x_{m,d}-x_{l,u}-x_{r_1,u}}\right).$$
$$\left(1+\frac{\tilde{\sigma}_{r_1 r_1}^2}{\sigma_{r_1 l}^2}e^{y_m+x_{r_1,d}-x_{l,u}}\right)\le\frac{1}{1-\epsilon_m}, \tag{28b}$$
$$R_m\le\log_2(1+e^{\bar{y}_m})+\frac{e^{\bar{y}_m}(y_m-\bar{y}_m)}{\ln 2(1+e^{\bar{y}_m})}, \tag{28c}$$
$$e^{x_{r_1,u}}\le P_{r_1}, \tag{28d}$$
$$e^{\bar{x}_{r_1,d}}(x_{r_1,d}-\bar{x}_{r_1,d}+1)\ge P_{r_1}, \tag{28e}$$
$$e^{x_{m,u}}\le P_m, \tag{28f}$$
$$e^{\bar{x}_{m,d}}(x_{m,d}-\bar{x}_{m,d}+1)\ge P_m, \tag{28g}$$
$$\{e^{x_{m,u}},e^{x_{m,d}},e^{x_{r_1,u}},e^{x_{r_1,d}}\}\in\Omega_p^s \text{ or } \Omega_p^i. \tag{28h}$$

As a result, the outage probability constraints may not hold with equality for $(\hat{R}_1,\hat{R}_2,\hat{x}_{m,u},\hat{x}_{m,d},\hat{x}_{r_1,u},\hat{x}_{r_1,d})$ for (28b). In this case, we can actually find a larger rate tuple $(\tilde{R}_1,\tilde{R}_2)$, where $\tilde{R}_m\ge\hat{R}_m, m=1,2$ by solving the following equations

$$\exp\left(\left(\frac{\tilde{\sigma}_{mm}^2}{\sigma_{r_1 m}^2}e^{\hat{x}_{m,d}-\hat{x}_{r_1,u}}+\frac{1}{\sigma_{r_1 m}^2}e^{-\hat{x}_{r_1,u}}+\frac{1}{\sigma_{r_1 l}^2}e^{-\hat{x}_{l,u}}+\right.\right.$$
$$\left.\left.\frac{\tilde{\sigma}_{mm}^2}{\sigma_{r_1 l}^2}e^{2\hat{x}_{m,d}-\hat{x}_{l,u}-\hat{x}_{r_1,u}}+\frac{1}{\sigma_{r_1 l}^2}e^{\hat{x}_{m,d}-\hat{x}_{l,u}-\hat{x}_{r_1,u}}\right)\left(2^{R_m}-1\right)\right)$$
$$\cdot\left(1+\frac{\tilde{\sigma}_{r_1 r_1}^2(2^{R_m}-1)}{\sigma_{r_1 l}^2}e^{\hat{x}_{r_1,d}-\hat{x}_{l,u}}\right)=\frac{1}{1-\epsilon_m}, \tag{29}$$

for $m=1,2,\ l\in\{1,2\}\setminus\{m\}$. Note that the equations in (29) can be efficiently solved by simple line search. Now, we can obtain $(\tilde{R}_1,\tilde{R}_2,\hat{x}_{m,u},\hat{x}_{m,d},\hat{x}_{r_1,u},\hat{x}_{r_1,d})$, which serves as an sub-optimal solution to problem (24). Note that $(\tilde{R}_1,\tilde{R}_2,\hat{x}_{m,u},\hat{x}_{m,d},\hat{x}_{r_1,u},\hat{x}_{r_1,d})$ is also a feasible point of problem (24). Therefore, we can use it to further construct first-order lower bounds and to obtain the corresponding convex approximate problem. Such procedure can be repeated successively to construct a SCA algorithm that improves the utility achieved by our solution iteratively.

The SCA algorithm halts at a predefined stopping criterion. We summarize the SCA algorithm for a TWRN with a single relay node in Algorithm 1.

Algorithm 1 SCA algorithm for problem (24)

1: **Given** $(\bar{P}_1,\bar{P}_2,\bar{P}_{r_1})\in\Omega_p^i$ or Ω_p^s and $(\bar{R}_1,\ \bar{R}_2)$ that are feasible to (24).
2: Set $\hat{P}_{m,d}[0]=\bar{P}_m$, $\hat{P}_{r_1,d}[0]=\bar{P}_{r_1}$, and $\tilde{R}_m[0]=\bar{R}_m$ for all $m=1,2$, and set $n=0$.
3: **repeat**
4: $n:=n+1$
5: Obtain $\bar{y}_m[n-1]=\ln(2^{\tilde{R}_m[n-1]}-1),\bar{x}_{m,d}[n-1]=\ln(\hat{P}_m[n-1])$, $\bar{x}_{r_1,d}[n-1]=\ln(\hat{P}_{r_1}[n-1])$ for $m=1,2$, and solve (28) to obtain optimal solution $\hat{\mathbf{u}}[n]\triangleq(\{\hat{R}_m[n]\},\{\hat{y}_m[n]\},\{\hat{x}_{m,u}[n]\},\{\hat{x}_{m,d}[n]\},\hat{x}_{r_1,u}[n],\hat{x}_{r_1,d}[n])$.
6: Compute $(\tilde{R}_1[n],\tilde{R}_2[n])$ by solving (29).
7: **until** the stopping criterion is met.
8: **Obtain** the optimal solution as $\mathbf{u}^*=(\{\tilde{R}_m[n]\},\{\hat{y}_m[n]\},\{\hat{x}_{m,u}[n]\},\{\hat{x}_{m,d}[n]\},\hat{x}_{r_1,u}[n],\hat{x}_{r_1,d}[n])$.

B. SCA Algorithm for Multiple Relay Nodes

In this subsection, we consider the utility maximization problem for a TWRN with multiple relay nodes under an individual and a sum power constraint. For a single relay node, we focus on power allocation problem between source nodes and the relay node. For multiple relay nodes, we focus on the power allocation problem among relay nodes. Thus, S_1 and S_2 are assumed to use full power. To begin with, we substitute approximate closed-form expressions of outage probabilities (20) into (8) and obtain a optimization problem for a TWRN with multiple relay nodes:

$$\max_{(\{P_{r_i}\}_{i=1}^K,R_1,R_2)\succeq 0} \quad U(R_1,R_2) \tag{30a}$$

$$\text{s.t.} \quad \prod_{i=1}^K\left(\left(1+\frac{P_{r_i}^2u_m\tilde{\sigma}_{r_i r_i}^2}{N_{r_i}\sigma_{r_i l}^2}\right)\prod_{j=1,j\neq i}^K\left(1+\frac{P_{r_i}P_{r_j}u_m\sigma_{r_j r_i}^2}{N_{r_i}\sigma_{r_i l}^2}\right)\cdot\right.$$
$$\left.\exp\left(\frac{P_{r_i}u_m}{N_{r_i}\sigma_{r_i l}^2}\right)\right)\le\frac{1}{1-\epsilon_m}, \tag{30b}$$
$$\{P_{r_1},\ldots,P_{r_K}\}\in\Omega_p^s \text{ or } \Omega_p^i, \tag{30c}$$

for $m = 1, 2,\ l \in \{1, 2\} \setminus \{m\}$. Note that u_m, for $m = 1, 2$ are functions of R_1, R_2 and $\{P_{r_i}\}_{i=1}^K$ as defined in Subsection (III-B). To apply the SCA algorithm, further approximations are needed. Specifically, we replace P_{r_i} by full power $\bar{P}_{r_i}$ in (17) to obtain $N_{r_i,c}$, which is an approximation to N_{r_i}. Substituting N_{r_i} by $N_{r_i,c}$ into (30), the approximate problem can be represented as

$$\max_{(\{P_{r_i}\}_{i=1}^K, R_1, R_2) \succeq 0} U(R_1, R_2) \tag{31a}$$

$$\text{s.t.} \prod_{i=1}^K \left(\left(1 + \frac{P_{r_i}^2 u_m \tilde{\sigma}_{r_i r_i}^2}{N_{r_i,c}\sigma_{r_i l}^2} \right) \prod_{j=1, j\neq i}^K \left(1 + \frac{P_{r_i} P_{r_j} u_m \sigma_{r_j r_i}^2}{N_{r_i,c}\sigma_{r_i l}^2} \right) \cdot \exp\left(\frac{P_{r_i} u_m}{N_{r_i,c}\sigma_{r_i l}^2} \right) \right) \leq \frac{1}{1-\epsilon_m}, \tag{31b}$$

$$\{P_{r_1}, \ldots, P_{r_K}\} \in \Omega_p^s \text{ or } \Omega_p^i. \tag{31c}$$

Following the same process as we used in Subsection (IV-A), we apply the following change of variables

$$e^{x_{r_i}} \triangleq P_{r_i}, e^{y_m} \triangleq 2^{R_m} - 1,$$
$$e^{z_m} \triangleq P_l \left(\sum_{k=1}^K \sqrt{\frac{P_{r_k}}{N_{r_k,c}}} \right)^2 - \left(2^{R_m} - 1 \right) \left(P_m \tilde{\sigma}_{mm}^2 + 1 \right), \tag{32}$$

for $i = 1, \ldots, K$, and $m = 1, 2,\ l \in \{1, 2\} \setminus \{m\}$, where $(\{x_{r_i}\}_{i=1}^K, y_1, y_2, z_1, z_2)$ are slack variables. Note that variables z_m are introduced such that $u_m = e^{y_m - z_m}$. Then, problem (31) can be derived as

$$\max_{\substack{(R_1,R_2)\succeq 0,\\ (\{x_{r_i}\}_{i=1}^K, y_m, z_m) \in \mathbb{R}^{K+4}}} U(R_1, R_2) \tag{33a}$$

$$\text{s.t.} \prod_{i=1}^K \left(\left(1 + \frac{\tilde{\sigma}_{r_i r_i}^2}{N_{r_i,c}\sigma_{r_i l}^2} e^{2x_{r_i} + y_m - z_m} \right) \prod_{j=1, j\neq i}^K \left(1 + \frac{\sigma_{r_j r_i}^2}{N_{r_i,c}\sigma_{r_i l}^2} e^{x_{r_i} + x_{r_j} + y_m - z_m} \right) \exp\left(\frac{1}{N_{r_i,c}\sigma_{r_i l}^2} e^{x_{r_i} + y_m - z_m} \right) \right) \leq \frac{1}{1-\epsilon_m}, \tag{33b}$$

$$P_l \left(\sum_{k=1}^K \sqrt{\frac{1}{N_{r_k,c}}} e^{\frac{x_{r_k}}{2}} \right)^2 - \left(1 + P_m \tilde{\sigma}_{mm}^2 \right) e^{y_m} \geq e^{z_m}, \tag{33c}$$

$$R_m \leq \log_2 \left(1 + e^{y_m} \right), \tag{33d}$$

$$\{e^{x_{r_1}}, \cdots, e^{x_{r_K}}\} \in \Omega_p^s \text{ or } \Omega_p^i, \tag{33e}$$

for $m = 1, 2,\ l \in \{1, 2\} \setminus \{m\}$. Note that we replace equalities with inequalities in (33c) and (33d), indicating relaxations of the original constraints. It can be verified by contradiction that inequality constraints (33b), (33c), and (33d) must hold with equalities at the optimal point. However, we can observe that the optimization problem (33) is still non-convex due to constraints (33c) and (33d). In order to tackle these non-convex constraints, we introduce a set of first-order approximations, which is a set of conservative approximations. To begin with, we let $(\{\bar{P}_{r_i}\}_{i=1}^K, \bar{R}_1, \bar{R}_2)$ be a feasible point of problem (33). Define

$$\bar{y}_m \triangleq \ln(2^{\bar{R}_m} - 1), \bar{x}_{r_i} \triangleq \ln(\bar{P}_{r_i}), \text{ for } i = 1, \ldots, K,\ m = 1, 2, \tag{34}$$

such that$(\bar{R}_1, \bar{R}_2, \{\bar{x}_{r_i}\}_{i=1}^K, \bar{y}_m)$ is feasible to problem (33). Now, the first-order approximation, which serves as a lower bound to the original function is applied to (33c) and (33d). Then, we obtain an approximate problem for (31), which can be represented as

$$\max_{\substack{(R_1,R_2)\succeq 0,\\ (\{x_{r_i}\}_{i=1}^K, y_1, y_2\\ , z_1, z_2) \in \mathbb{R}^{K+4}}} U(R_1, R_2) \tag{35a}$$

$$\text{s.t.} \prod_{i=1}^K \left(\left(1 + \frac{\tilde{\sigma}_{r_i r_i}^2}{N_{r_i,c}\sigma_{r_i l}^2} e^{2x_{r_i} + y_m - z_m} \right) \prod_{j=1, j\neq i}^K \left(1 + \frac{\sigma_{r_j r_i}^2}{N_{r_i,c}\sigma_{r_i l}^2} e^{x_{r_i} + x_{r_j} + y_m - z_m} \right) \exp\left(\frac{1}{N_{r_i,c}\sigma_{r_i l}^2} e^{x_{r_i} + y_m - z_m} \right) \right) \leq \frac{1}{1-\epsilon_m}, \tag{35b}$$

$$P_l \left(\sum_{k=1}^K \sqrt{\frac{1}{N_{r_k,c}}} e^{\frac{\overline{x}_{r_k}}{2}} \right) \left(\sum_{k=1}^K \sqrt{\frac{1}{N_{r_k,c}}} e^{\frac{\overline{x}_{r_k}}{2}} \left(x_{r_k} - \overline{x}_{r_k} + 1 \right) \right) \geq e^{z_m} + \left(1 + P_m \tilde{\sigma}_{mm}^2 \right) e^{y_m}, \tag{35c}$$

$$R_m \leq \log_2(1 + e^{\bar{y}_m}) + \frac{e^{\bar{y}_m}(y_m - \bar{y}_m)}{\ln 2 \cdot (1 + e^{\bar{y}_m})}, \tag{35d}$$

$$\{e^{x_{r_1}}, \cdots, e^{x_{r_K}}\} \in \Omega_p^s \text{ or } \Omega_p^i. \tag{35e}$$

for $m = 1, 2,\ l \in \{1, 2\} \setminus \{m\}$. Problem (35) is now a convex optimization problem. Thus, it can be solved by CVX. We let $(\hat{R}_1, \hat{R}_2, \{\hat{x}_{r_i}\}_{i=1}^K, \hat{z}_m)$ denote the optimal solution to problem (35). Since the first-order approximation is a conservative approximation, we can further obtain $\tilde{R}_m \geq \hat{R}_m$, $m = 1, 2$ by solving the following equations

$$\prod_{i=1}^K \left(\left(1 + \frac{\tilde{\sigma}_{r_i r_i}^2 (2^{R_m} - 1)}{N_{r_i,c}\sigma_{r_i n}^2} e^{2\hat{x}_{r_i} - \hat{z}_m} \right) \prod_{j=1, j\neq i}^K \left(1 + \frac{\sigma_{r_j r_i}^2 (2^{R_m} - 1)}{N_{r_i,c}\sigma_{r_i n}^2} e^{\hat{x}_{r_i} + \hat{x}_{r_j} - \hat{z}_m} \right) \exp\left(\frac{(2^{R_m} - 1)}{N_{r_i,c}\sigma_{r_i n}^2} e^{\hat{x}_{r_i} - \hat{z}_m} \right) \right) = \frac{1}{1-\epsilon_m}, \tag{36}$$

for $m = 1, 2,\ l \in \{1, 2\} \setminus \{m\}$. We can use simple line search to solve the equations as before. Then, we can obtain an approximate solution $(\tilde{R}_1, \tilde{R}_2, \{\hat{x}_{r_i}\}_{i=1}^K, \hat{z}_m)$ to problem (31). Note that $(\tilde{R}_1, \tilde{R}_2, \{\hat{x}_{r_i}\}_{i=1}^K, \hat{z}_m)$ is also a feasible point of problem (31). Therefore, we can use it to further construct first-order lower bounds and to obtain the correspond convex approximate problem. Such procedure can be repeated successively to construct a SCA algorithm that improves the utility achieve by our solution iteratively. Note that (35) is a convex approximation to (31), not to the original problem (30). Thus, we further use line search on R_1 and R_2 to obtain the actual achieve rate tuple $(R_1^*[n], R_2^*[n])$ to (30) based on the optimal power allocation $(\hat{P}_{r_1}, \cdots, \hat{P}_{r_K})$ obtained from (35). The resulting SCA algorithm for a TWRN with multiple relay nodes is summarized in Algorithm 2.

The convergence of Algorithm 1 and Algorithm 2 can be proved using similarly arguments as in [23]. Note that the SCA algorithm only guarantees to converge to local optimal points, the selection of initial points has an impact on its ability to converge to the global optimal point.

V. Simulation Results

In this section, we demonstrate the performance of our proposed SCA algorithm for solving the utility optimization problem for a TWRN with a single relay node and multiple relay nodes under an individual and a sum power constraint. In all simulations, the channel coefficients are assumed to be i.i.d. Rayleigh random variables. The variance of the residual self-interference at source and relay nodes are assumed to be 0.01

This article has been accepted for publication in a future issue of this journal, but has not been fully edited. Content may change prior to final publication. Citation information: DOI 10.1109/TSP.2017.2736507, IEEE Transactions on Signal Processing

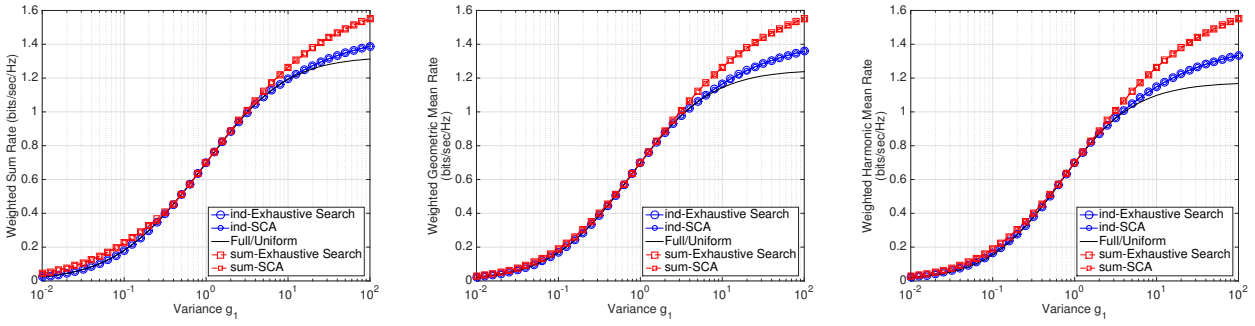

(a) (b) (c)

Fig. 3: Simulation results of different utility functions versus the variance of g_1 with a single relay node, and $(\alpha_1, \alpha_2) = (\frac{1}{2}, \frac{1}{2})$; (a) weighted sum rate, (b) weighted geometric mean rate, (c) weighted harmonic mean rate.

Algorithm 2 SCA algorithm for problem (30)

1: **Approximate** problem (30) to problem (31).
2: **Given** $(\bar{P}_{r_1}, \cdots, \bar{P}_{r_K}) \in \Omega_p^i$ or Ω_p^s and $(\bar{R}_1, \bar{R}_2)$ that are feasible to (31).
3: Set $\hat{P}_{r_i}[0] = \bar{P}_{r_i}$ and $\tilde{R}_m[0] = \bar{R}_m$ for all $i = 1, \cdots, K,\ m = 1, 2$, and set $n = 0$.
4: **repeat**
5: $n := n + 1$
6: Obtain $\bar{y}_m[n-1] = \ln(2^{\tilde{R}_m}[n-1] - 1), \bar{x}_{r_i}[n-1] = \ln(\hat{P}_{r_i}[n-1])$, for $i = 1, \ldots, K,\ m = 1, 2$, and solve problem (35) to obtain the optimal solution $\hat{\mathbf{u}}[n] \triangleq (\{\hat{R}_m[n]\}, \{\hat{x}_{r_i}[n]\}, \{\hat{y}_m[n]\}, \{\hat{z}_m[n]\})$.
7: Compute $(\tilde{R}_1[n], \tilde{R}_2[n])$ by solving (36).
8: **until** the stopping criterion is met.
9: **Obtain** the approximate optimal solution as $\tilde{\mathbf{u}} = (\{\tilde{R}_m[n]\}, \{\hat{x}_{r_i}[n]\}, \{\hat{y}_m[n]\}, \{\hat{z}_m[n]\})$ and correspond $(\hat{P}_{r_1}, \cdots, \hat{P}_{r_K})$.
10: According to $(\hat{P}_{r_1}, \cdots, \hat{P}_{r_K})$, **obtain** the actual achieve $\{R_m^*[n]\}$ rate to problem (30).
11: **Obtain** the optimal solution as $\mathbf{u}^* = (\{R_m^*[n]\}, \hat{P}_{r_1}, \cdots, \hat{P}_{r_K})$.

and 0.05, respectively. The variance of cross-link interference channel is assumed to be 0.1. The *channel truncation level* η is assumed to be 0.001. The outage probability requirement is set to 0.1 for the two source nodes, i.e., $\epsilon_1 = \epsilon_2 = 0.1$. The stopping criterion for the SCA algorithm is

$$\frac{|U(\tilde{R}_1[n], \tilde{R}_2[n]) - U(\tilde{R}_1[n-1], \tilde{R}_2[n-1])|}{U(\tilde{R}_1[n-1], \tilde{R}_2[n-1])} < 0.01,$$

which means that the algorithm stops if the improvement in the system utility is less than 1%. The initial point for the SCA algorithm is generated through the full power scheme. We use the convex solver `CVX` [29] to solve the approximate convex problems successively in the SCA algorithm.

A. Single Relay Node

In this subsection, we investigate the performance of our proposed SCA algorithm for a single relay node. We demonstrate the performance of different utility functions achieved by our proposed SCA algorithm under different degree of channel asymmetry. The variance of f_1 is set to 1, and the variance of g_1 varies from 0.01 to 100, representing different degree of channel asymmetry. We fix the peak power constraint of relay node and source nodes to be 30 W under the individual power constraint. We also let the total power constraint be 90 W for fair comparison. The full power scheme and uniform power scheme achieve the same performance under this setting. In Fig. 3(a)-(c), we can observe that the performance of our proposed SCA algorithm is similar to that of the exhaustive search method for all degree of channel asymmetry and utility functions. As shown in Fig. 3(a), the performance gap between the SCA algorithm and naive scheme is small when the channel is symmetric as expected. Note that the performance gap becomes much more evident when g_1 becomes stronger. In fact, the SCA algorithm allocates less power to S_2 when g_1 is strong under an individual power constraint. Allocating less power to S_2 reduces the achievable rate received at S_1 but the residual self-interference at S_2 is reduced simultaneously. When g_1 is strong, reducing the residual self-interference has a stronger impact on the achievable rate received at S_2 and hence the overall system utility. The same phenomenon can be observed for the sum power constraint. Since it is more flexible to allocate power between the source and the relay node for the sum power constraint, the performance gap is much larger between the SCA algorithm and naive scheme when the variance of g_1 increases. Similar trends can be observed in Fig. 3(b) and Fig. 3(c) for weighted geometric mean rate and weighted harmonic mean rate utility, respectively. When user fairness is more emphasized, we can observe that the gap between our proposed SCA algorithm and naive scheme also grow larger when the variance of g_1 increases.

In Fig. 4, we compare the total power consumption achieved by different schemes introduced in Fig. 3. In contrast to the limited performance improvement observed in Fig. 3(a)-(c) when g_1 is weak, there is significant saving in power consumption for all considered system utilities in Fig. 4(a)-(c). Specifically, the saving can be as high as 22%, 24%, and 27% when the variance of g_1 is equal to 10^{-2} for weighted sum, weighted geometric mean, and weighted harmonic mean rate, respectively. When g_1 is strong, we can also observe similar reduction in total transmitted power. This implies that judicious power allocation not only improves energy efficiency but also improves system utilities when g_1 is strong. Note that when user fairness is more emphasized, the saving in power

This article has been accepted for publication in a future issue of this journal, but has not been fully edited. Content may change prior to final publication. Citation information: DOI 10.1109/TSP.2017.2736507, IEEE Transactions on Signal Processing

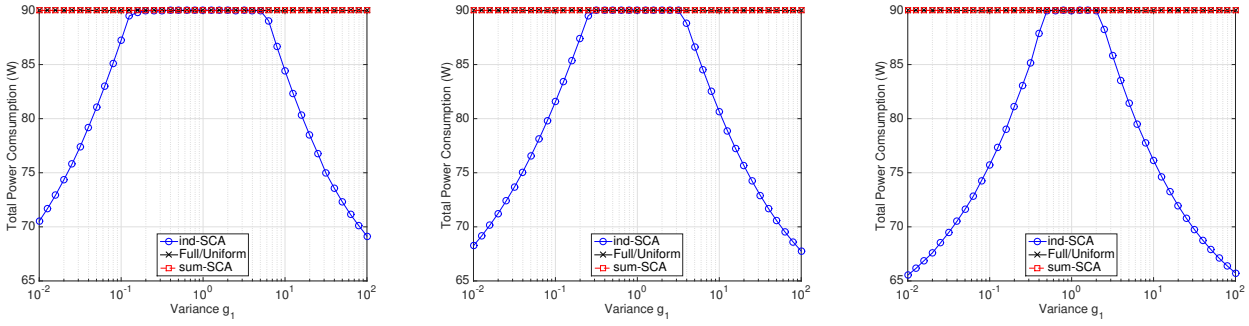

Fig. 4: Simulation results of the total power consumption versus the variance of g_1 with a single relay node; (a) weighted sum rate, (b) weighted geometric mean rate, (c) weighted harmonic mean rate.

consumption is even more evident, as observed in Fig. 4(b) and Fig. 4(c).

B. Multiple Relay Nodes

For a TWRN with multiple relay nodes, we focus on the power allocation problem among relay nodes. Thus, we set the power of S_1 and S_2 to 30 W. To observe the power allocation clearly, we consider the number of relay nodes as $K = 2$. For fair comparison, each relay node has a peak power budget of 30 W under the individual power constraint, and a total power budget of 60 W for all relay nodes under the sum power constraint. The full power scheme and uniform power scheme are the same under this setting. In Fig. 5, we demonstrate the performance of weighted sum, weighted geometric mean, and weighted harmonic mean rate with respect to the variance of g_1, which varies from 0.01 to 100. Note that g_1 is the channel from the first relay node to S_2. The variance of g_2 is fixed and and set to 1.

We can observe that the performance of our proposed SCA algorithm almost overlaps with that of the exhaustive search method for all degree of channel asymmetry and all utility functions, indicating that our proposed SCA algorithm achieves near-optimal performance. Different from the case of a single node, there is a obvious performance gap between our proposed SCA algorithm and the naive scheme in Fig. 5(a). The performance gap is about 14% when the variance of g_1 is equal to 1. This is because the SCA algorithm allocates less power to each relay node to avoid large cross-link interference between relay node, resulting in the observed performance improvement. Note that when the degree of channel asymmetry increases, the performance gap becomes even larger. The SCA algorithm now allocates most power to the relay node with the best channel strength. The system utility is improved by utilizing the better channel link, and reducing cross-link interference at the same time. Again, the flexibility offered by the sum power constraint allows the allocation of more power to the user with the best channel strength. This leads to additional performance gain especially when the variance of g_1 is large. In Fig. 5(b) and Fig. 5(c), similar performance gaps can be observed for weighted geometric mean rate and weighted harmonic mean rate when user fairness is considered.

In Fig. 6, we compare the power consumption for different schemes discussed in Fig. 5. Focusing on P_{r_1} and P_{r_2} in Fig. 6(a) under the individual power constraint, we observe that the SCA algorithm allocates less power to each relay node to lower cross-link interference than the naive scheme when we have symmetric channels. When the degree of channel asymmetry increases, the SCA algorithm allocates more power to the relay node with a stronger channel and less power to the other relay node to prevent the cross-link interference becoming larger under the individual power constraint. The same phenomenon can be observed for the sum power constraint. Note that only modest power (40 W) is allocated by the SCA algorithm to the second relay node when g_1 is weak. If P_{r_2} is too large, the overall system utility suffers since the residual self-interference also become larger. However, the SCA algorithm allocates almost full power to the first relay node when g_1 is strong. Although a large P_{r_1} causes strong residual self-interference, the channel g_1 is strong enough to overcome the residual self-interference and improve the achievable rate received at S_2. In Fig. 6(b) and Fig. 6(c), when the user fairness is considered, the SCA algorithm would allocate less power to the first relay node to achieve a more balanced rate at S_1 and S_2 when g_1 is strong.

C. Comparison with a Relay Selection Scheme

In this subsection, we compare performance between our proposed SCA algorithm and a relay selection scheme for a TWRN with with multiple relay nodes. We consider the number of relay nodes as $K = 3$ here. The relay selection scheme we consider here select the relay with the strongest channel gain. In Fig. 7(a), we compare the weighted sum rates achieved by different schemes with respect to the variance of g_1. Note that only the variance of g_1 is varied here. The variances of the other channels are all set to 1. In contrast, the variances of all $\{g_i\}_{i=1}^3$ are changed simultaneously in Fig. 7(b). The powers of S_1 and S_2 are fixed to 30 W, and the total power constraint of all the relay nodes is set to 30 W, i.e, the power constraint of each relay node is set to 10 W.

In Fig. 7(a)(b), we observe that the performance of our proposed SCA algorithm almost matches perfectly with that

This article has been accepted for publication in a future issue of this journal, but has not been fully edited. Content may change prior to final publication. Citation information: DOI 10.1109/TSP.2017.2736507, IEEE Transactions on Signal Processing

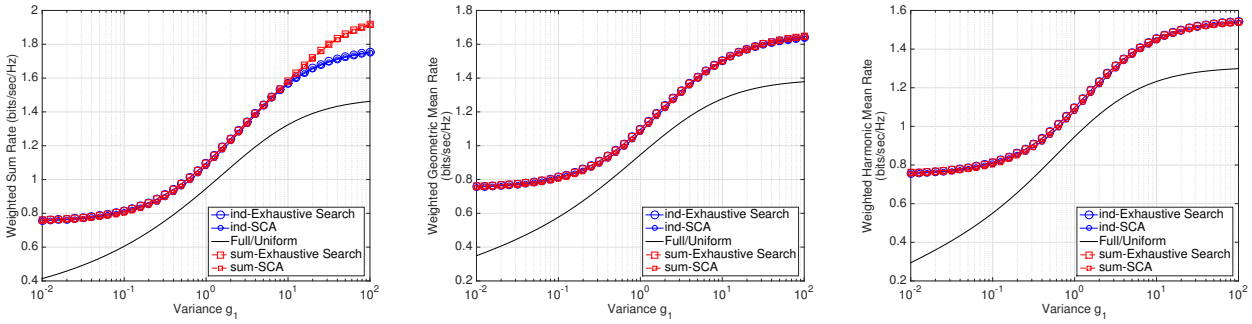

(a) (b) (c)

Fig. 5: Simulation results of different utility functions versus the variance of g_1 with multiple relay nodes, and $(\alpha_1, \alpha_2) = (\frac{1}{2}, \frac{1}{2})$; (a) weighted sum rate, (b) weighted geometric mean rate, (c) weighted harmonic mean rate.

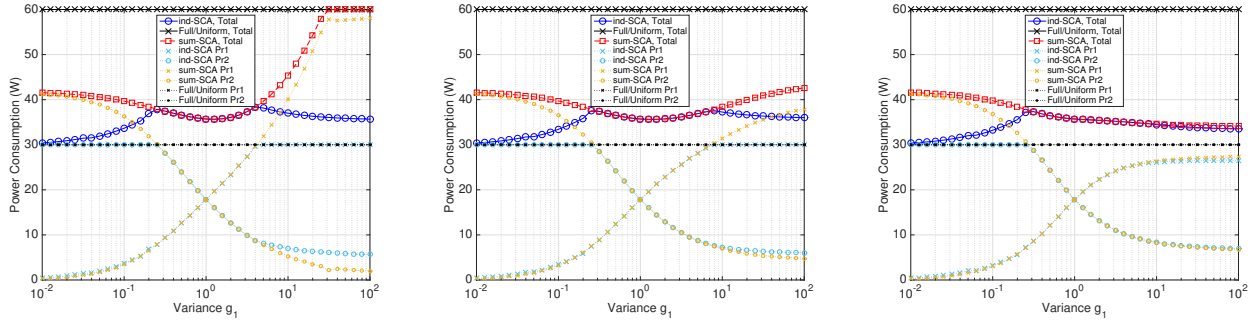

(a) (b) (c)

Fig. 6: Simulation results of the power consumption versus the variance of g_1 with multiple relay nodes; (a) weighted sum rate, (b) weighted geometric mean rate, (c) weighted harmonic mean rate.

achieved by the exhaustive search method. Our proposed SCA algorithm also achieves near-optimal performance for $K = 3$. In Fig 7(a), we can observe that the SCA algorithm is uniformly better than relay selection for both power constraints. When channel is symmetric, the SCA algorithm would allocate powers to multiple relay nodes simultaneously. The performance gain is as high as 174% between the SCA algorithm and the relay selection scheme when the variance of g_1 is 1 under the individual power constraint, and 85% under the sum power constraint. When channel is asymmetric, the SCA algorithm not only allocates power to the stronger channel but also judiciously allocates modest powers to the other relay nodes to increase performance under the individual power constraint. The same phenomenon can be observed for the sum power constraint. In Fig. 7(b), there is a difference between the SCA algorithm and the relay selection scheme regardless of channel conditions or power constraints. The SCA algorithm is uniformly better than relay selection. This is because the SCA algorithm can use multiple relay nodes simultaneously, and the advantage would become more obvious when the variance of g_i, $\forall\ i$ increases. The curves of the SCA algorithm under an individual and a sum power constraint are the same. The reason is that when the channel conditions of the first relay node and the second relay node are almost the same, the SCA algorithm would allocate power equally to both relay nodes.

D. Comparsion between a HD and a FD

We compare the weighted sum rate utility with respect to residual self-interference in Fig. 8(a) and cross-link interference in Fig. 8(b). We consider the number of relay nodes as $K = 3$. The power setting is the same as that in Fig. 7(b). The variance of g_i and f_i are set to 1 for $i = 1, 2, 3$. Note that the SCA algorithm for a HD system would allocate full power equally to all relay nodes. Thus, the utility achieved by the SCA algorithm is the same under the individual and sum power constraint for a HD system. In Fig. 8(a), we can observe a tradeoff in performance between the HD and FD system. The FD system outperforms the HD system when the variance of residual self-interference channel is less than 0.25. In Fig. 8(b), a similar tradeoff can be observed when the cross-link interference increases. The FD system achieves a higher utility when the variances of cross-link interference channels are less than 0.2. We can observe that not only the residual self-interference but also cross-link interference is a factor that degrades the system performance for a FD system. Note that when the cross-link interference is large, we can observe that the SCA algorithm achieves a higher utility under the sum power constraint. This is because when the variance of cross-

This article has been accepted for publication in a future issue of this journal, but has not been fully edited. Content may change prior to final publication. Citation information: DOI 10.1109/TSP.2017.2736507, IEEE Transactions on Signal Processing

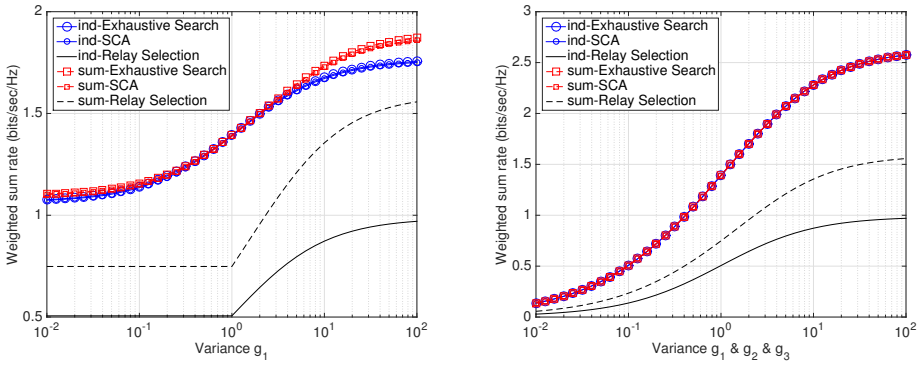

(a) (b)

Fig. 7: Simulation results of the comparison between the SCA algorithm and the relay selection scheme for multiple relay nodes, and $(\alpha_1, \alpha_2) = (\frac{1}{2}, \frac{1}{2})$; (a) weighted sum rate versus the variance of g_1 (b) weighted sum rate versus the variance of g_1, g_2, and g_3 simultaneously.

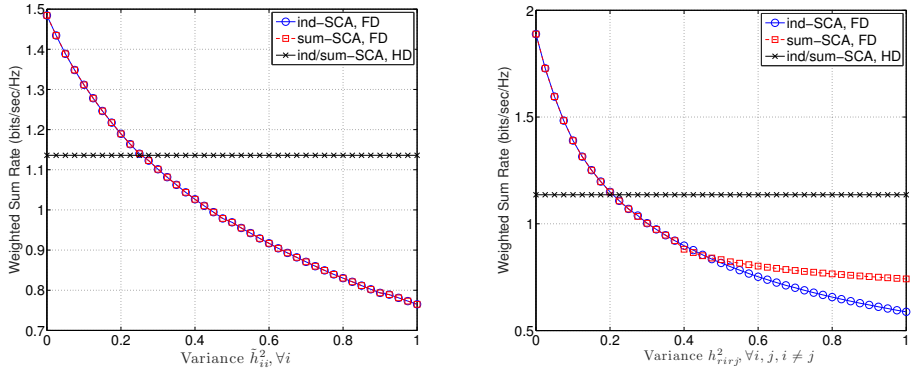

(a) (b)

Fig. 8: Simulation results of the tradeoff between HD and FD for multiple relay nodes, and $(\alpha_1, \alpha_2) = (\frac{1}{2}, \frac{1}{2})$; (a) weighted sum rate versus the variance of $\tilde{h}^2_{r_i r_i}$, for $i = 1, 2, 3$, (b) weighted sum rate versus the variance of $h^2_{r_j r_i}$, for $i, j = 1, 2, 3$ $i \neq j$.

link increases, the SCA algorithm tends to allocate most power to one relay node. More power can be allocated to a single relay node under the sum power constraint than under the individual power constraint.

VI. Conclusion

In this study, we investigate the optimal power allocation that maximizes a general utility function for a FD-AF relaying TWRN under a rate outage constraint and a power constraint. Either an individual power constraint or a sum power constraint is considered. To solve the utility maximization problem, we derive two different approximate closed-form expressions of outage probabilities, one for a TWRN with a single relay node and the other for multiple relay nodes. The approximation accuracy for both expressions were verified by extensive Monte Carlo simulations. However, based on the derived expressions, the resulting optimal problems are still non-convex and difficult to solve. For this, we applied convex approximation techniques, including change of variables and first-order approximations, to obtain a series of convex approximation problems. By solving this series of convex problems successively, we proposed the SCA algorithms for a TWRN with a single relay node and multiple relay nodes, respectively. Finally, our simulation results demonstrate that the power allocations provided by the proposed SCA algorithms yield near-optimal performance when compared with the exhaustive search method. To emphasize the importance of power allocation in FD-AF relaying TWRN, we compare the utility and power consumption achieved by the SCA algorithms with the naive schemes, when full power or uniform power is applied. While our proposed SCA algorithm achieve significant reduction in power consumption for a TWRN with a single relay node, we observed significant advantages both in achieved system utility and in consumed power by our proposed SCA algorithm over the naive scheme when there are multiple relay nodes in a TWRN. Our results show that proper power allocation is essential, especially when there are multiple relay nodes in the system. For our proposed SCA algorithm, powers are allocated to mutliple relay nodes to transmit simultaneously. When compared with the relay

selection scheme where only one relay is allowed to transmit at a time, the utility achieved by the SCA algorithm was shown to improve by as large as 174% under the individual power constraint and 85% under the sum power constraint when the channel is symmetric. Our FD system was further compared with a HD system. Our simulations demonstrate a tradeoff between the FD and HD system with respect to the residual self-interference as expected. We can also observe that not only the residual self-interference but also the cross-link interference is a fact that degrades the system performance for a FD system.

REFERENCES

[1] J. N. Laneman, D. N. C. Tse, and G. W. Wornell, "Cooperative diversity in wireless networks: Efficient protocols and outage behavior," *IEEE Trans. Inf. Theory*, vol. 50, no. 12, pp. 3062–3080, December 2004.

[2] T. M. COVER and A. A. E. GAMAL, "Capacity theorems for the relay channel," *IEEE Trans. Inf. Theory*, vol. 25, no. 5, pp. 572–584, Sept 1979.

[3] G. Kramer, M. Gastpar, and P. Gupta, "Cooperative strategies and capacity theorems for relay networks," *IEEE Trans. Inf. Theory*, vol. 51, no. 9, pp. 3037–3063, Sept 2005.

[4] Y. Ni, X. Wang, S. Jin, K.-K. Wong, H. Zhu, and N. Zhang, "Outage probability of device-to-device communication assisted by one-way amplify-and-forward relaying," *IET Communications*, vol. 9, pp. 271–282, Sept 2014.

[5] W. Xu and X. Dong, "Optimized one-way relaying strategy with outdated csi quantization for spatial multiplexing," *IEEE Trans. Signal Process.*, vol. 60, no. 8, pp. 4458–4464, August 2012.

[6] Y. Jing and H. Jafarkhani, "Network beamforming using relays with perfect channel information," *IEEE Transactions on Information Theory*, pp. 2499–2517, 2009.

[7] S. Katti, S. Gollakota, and D. Katabi, "Embracing wireless interference: Analog network coding," *ACM 2007 Article*, vol. 37, pp. 397–408, October 2007.

[8] Y. Li and F.-C. Zheng, "Relay selection and power allocation in analogue network coding system with asymmetric traffic under imperfect csi," *IEEE Global Communications Conference (GLOBECOM)*, pp. 4713 – 4718, December 2012.

[9] S. Talwar and S. ShahbazPanahi, "A total power minimization approach to relay selection for two-way relay networks," *Conference Record of the Forty Sixth Asilomar Conference on Signals, Systems and Computers (ASILOMAR)*, pp. 2001 – 2005, November 2012.

[10] M. Zeng, R. Zhang, and S. Cui, "On design of collaborative beamforming for two-way relay networks," *IEEE Trans. Signal Process.*, vol. 59, no. 5, pp. 2284–2295, May 2011.

[11] C.-L. Chen and C. Lin, "Utility maximization for two-way af relaying under rate outage constraints," *submitted to IEEE Trans. Signal Process.*

[12] D. W. Bliss, P. A. Parker, and A. R. Margetts, "Simultaneous transmission and reception for improved wireless network performance," *2007 IEEE/SP 14th Workshop on Statistical Signal Processing*, pp. 478 – 482, 2007.

[13] H. Ju, E. Oh, and D. Hong, "Improving efficiency of resource usage in two-hop full duplex relay systems based on resource sharing and interference cancellation," *IEEE Trans. Wireless Commun.*, vol. 8, no. 8, pp. 3933–3938, August 2009.

[14] A. E. Gamal and Y.-H. Kim, *Network Information Theory*, January 2012.

[15] M. Duarte, C. Dick, and A. Sabharwal, "Experiment-driven characterization of full-duplex wireless systems," *IEEE Trans. Wireless Commun.*, vol. 11, no. 12, pp. 4296–4307, December 2012.

[16] Y. Hua, P. Liang, Y. Ma, A. C. Cirik, and Q. Gao, "A method for broadband full-duplex mimo radio," *IEEE Signal Process. Lett*, vol. 19, no. 12, pp. 793–796, December 2012.

[17] W. Lee, "The most spectrum-efficient duplexing system: Cdd," *IEEE Commun. Mag.*, vol. 40, no. 3, pp. 163 – 166, March 2002.

[18] T. Riihonen, S. Werner, and R. Wichman, "Hybrid full-duplex/half-duplex relaying with transmit power adaptation," *IEEE Trans. Wireless Commun.*, vol. 10, no. 9, pp. 3074–3085, Sept 2011.

[19] L. J. Rodrguez, N. H. Tran, and T. Le-Ngoc, "Optimal power allocation and capacity of full-duplex af relaying under residual self-interference," *IEEE Wireless Commun. Lett.*, vol. 3, no. 2, pp. 233–236, Apr. 2014.

[20] H. Cui, M. Ma, L. Song, and B. Jiao, "Relay selection for two-way full duplex relay networks with amplify-and-forward protocol," *IEEE Trans. Signal Process.*, vol. 13, no. 7, pp. 3768–3777, July 2014.

[21] B. Zhong and Z. Zhang, "Opportunistic two-way full-duplex relay selection in underlay cognitive networks," *IEEE Systems Journal*, pp. 1–10, January 2016.

[22] I. Krikidis, H. A. Suraweera, P. J. Smith, and C. Yuen, "Full-duplex relay selection for amplify-and-forward cooperative networks," *IEEE Trans. Wireless Commun.*, vol. 11, no. 12, pp. 4381–4392, December 2012.

[23] W.-C. Li, T.-H. Chang, C. Lin, and C.-Y. Chi, "Coordinated beamforming for multiuser miso interference channel under rate outage constraints," *IEEE Trans. Signal Process.*, vol. 61, no. 5, pp. 1087–1103, March 2013.

[24] K. Alexandris, A. Balatsoukas-Stimming, and A. Burg, "Measurement-based characterization of residual self-interference on a full-duplex mimo testbed," *IEEE 8th Sensor Array and Multichannel Signal Processing Workshop (SAM)*, pp. 329–332, June 2014.

[25] *Full-Duplex wireless: Design, implementation and characterization*. Melissa Duarte, 2012.

[26] G. Zheng, "Joint beamforming optimization and power control for full-duplex mimo two-way relay channel," *IEEE Transactions on Signal Processing*, vol. 63, pp. 555–566, December 2015.

[27] J. Mo and J. Walrand, "Fair end-to-end window-based congestion control," *IEEE/ACM Trans. Netw.*, vol. 8, no. 5, pp. 556–567, October 2000.

[28] H. Bagheri, M. Ardakani, and C. Tellambura, "Power allocation for two-way amplify-forward relaying with receive channel knowledge," *IEEE 22nd International Symposium on Personal, Indoor and Mobile Radio Communicatio*, pp. 1708–1712, 2011.

[29] M. Grant and S. Boyd, "Cvx: Matlab software for disciplined convex programing , version 2.0," http://cvxr.com/cvx, Apr. 2011.

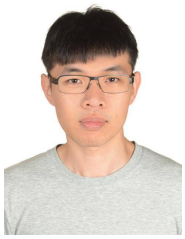

Jyun-Wei Li received the B.S degree in electrical engineering from Chung Yuan Christian University (CYCU), Taoyuan, Taiwan, in 2011, and the M.S. degree in communications engineering at the National Tsing Hua University (NTHU), Hsinchu, Taiwan, in 2016. His research interests include digital signal processing, wireless relay networks, optimization theory. Now, he works in Fareastone.

Che Lin (S02-M08-SM'16) received the B.S. degree in Electrical Engineering from National Taiwan University, Taipei, Taiwan, in 1999. He received the M.S. degree in Electrical and Computer Engineering in 2003, the M.S. degree in Math in 2008, and the Ph.D. degree in Electrical and Computer Engineering in 2008, all from the University of Illinois at Urbana-Champaign, IL. In 2008, he joined the Department of Electrical Engineering at National Tsing Hua University as an assistant professor, and has been an associate professor since August 2014.

Dr. Lin received a two-year Vodafone graduate fellowship in 2006, the E. A. Reid fellowship award in 2008, and holds a U.S. patent, which has been included in the 3GPP LTE standard. In 2012, he received the Excellent Teaching Award for the college of EECS, NTHU. He won the best paper award for 2014 GIW-ISCB-ASIA conference. In 2015, he received the CIEE outstanding young electrical engineer Award. He is a senior member of IEEE.

His research interests include deep learning, data mining and analytic, signal processing in wireless communications, optimization theory, and systems biology.